



Comparative Morphology of Dorsanum miran and Bullia granulosa from Morocco (Mollusca: Caenogastropoda: Nassariidae)

Authors: Simone, Luiz Ricardo L., and Pastorino, Guido

Source: African Invertebrates, 55(1) : 125-142

Published By: KwaZulu-Natal Museum

URL: <https://doi.org/10.5733/afin.055.0107>

BioOne Complete (complete.BioOne.org) is a full-text database of 200 subscribed and open-access titles in the biological, ecological, and environmental sciences published by nonprofit societies, associations, museums, institutions, and presses.

Your use of this PDF, the BioOne Complete website, and all posted and associated content indicates your acceptance of BioOne's Terms of Use, available at www.bioone.org/terms-of-use.

Usage of BioOne Complete content is strictly limited to personal, educational, and non - commercial use. Commercial inquiries or rights and permissions requests should be directed to the individual publisher as copyright holder.

BioOne sees sustainable scholarly publishing as an inherently collaborative enterprise connecting authors, nonprofit publishers, academic institutions, research libraries, and research funders in the common goal of maximizing access to critical research.

Comparative morphology of *Dorsanum miran* and *Bullia granulosa* from Morocco (Mollusca: Caenogastropoda: Nassariidae)

Luiz Ricardo L. Simone¹ and Guido Pastorino²

¹Museu de Zoologia da Universidade de São Paulo, Cx. Postal 42494, 04299-970 São Paulo, SP, Brazil; lrsimone@usp.br, lrlsimone@gmail.com

²Museo Argentino de Ciencias Naturales “Bernardino Rivadavia”, Av. Angel Gallardo 470 3 piso lab. 80, C1405DJR Ciudad Autónoma de Buenos Aires, Argentina; gpastorino@macn.gov.ar

ABSTRACT

The anatomy and taxonomy of two western African nassariids are explored, based on samples collected in Morocco. The species are *Dorsanum miran*, the type species of the genus, and *Bullia granulosa*, a characteristic member of *Bullia*. Both possess the typical morphological and anatomical features of the family, including a pair of metapodial tentacles, a well-developed proboscis, elongated odontophore with fusion of cartilages, and highly concentrated central nervous system. Both species have in common the socket-like heads, bifid columellar muscles, and reduction of the gland of Leiblein. *D. miran* has well-developed eyes, cement gland, and preputial protection at the penis tip. *B. granulosa* lacks eyes, has multiplicity of some buccal mass muscles (transverse muscles and main dorsal tensor muscles – m2), and a thick-walled and broad anterior oesophagus. The characters are discussed in the light of present knowledge concerning caenogastropod taxonomy.

KEY WORDS: Mollusca, Caenogastropoda, Buccinoidea, *Bullia*, *Dorsanum*, Morocco, morphology, taxonomy, classification.

INTRODUCTION

This paper is part of a project reviewing the South American species usually included in the region's nassariid genus *Buccinanops* d'Orbigny, 1841. Since the original description, the species of *Buccinanops* have been included in several different genera (Pastorino 1993). Two of the most used, *Dorsanum* Gray, 1847 and *Bullia* Gray, 1834 (in Griffith & Pidgeon 1834), both originally described from Africa, have some taxonomic problems associated with them and they are poorly defined at the anatomical level. The most recent and comprehensive revisions of these genera were published more than two decades ago. Adam and Knudsen (1984) regarded *Dorsanum* as a junior synonym of *Bullia*. Allmon (1990) considered *Dorsanum* to be valid, but restricted to the type species only, i.e., *D. miran* (Bruguère, 1789). In that paper, he introduced the subfamily Bulliinae to include *Bullia*, with *Buccinanops* as a subgenus, and *Dorsanum*. Pastorino (1993) re-established the full generic status of *Buccinanops* for all South American species, but a more complete discussion on the genera *Bullia* and *Dorsanum* is still wanting. Only a few papers (e.g. Simone 1996, 2011) describe the anatomy of soft parts of these taxa and all of those descriptions have been restricted so far to South American species.

These three genera were included by Brown (1982) in what he called the “*Bullia* group”. Later, Allmon (1990) extended this informal group, as Bulliinae, to fossil species, mostly from North America. He defined three subfamilies in Nassariidae: Nassariinae, Dorsaninae and Bulliinae. He included in Bulliinae a set of nassariids of relatively large size, having thin-walled shells, and confined to temperate and subtropical waters in the mid and south Atlantic and Indian Oceans. Dorsaninae is restricted to *Dorsanum*, while the genera *Bullia* (from Africa) and *Buccinanops* (from South America) comprise the Bulliinae. Despite these definitions, the differences amongst the subfamilies remain

<http://africaninvertebrates.org>

urn:lsid:zoobank.org:pub:4D7F54FA-2DD2-466A-9D47-FA1F6739F129

somewhat unclear. It is quite possible that additional information on their representatives, in terms of anatomy, could bring new insights, as the shell characters so far invoked have been insufficient to define the subfamilies and are not applicable to all included species.

As regards this scenario, the present paper deals with two species from the western coast of Africa: *Dorsanum miran*, type species of *Dorsanum*, and *Bullia granulosa* (Lamarck, 1822). Both are formally redescribed, including consideration of previously neglected anatomical aspects. Provision of the new information explored here has the target of laying a better foundation for future discussions and analysis concerning monophyly, and the phylogenetic and taxonomic allocation of the “*Bullia* group” (Brown 1982) and the Bulliinae/Dorsaninae (Allmon 1990), as well as the included genera *Bullia*, *Dorsanum* and *Buccinanops*. However, the present paper is almost purely descriptive, with discussion limited to data published so far.

MATERIAL AND METHODS

Most of the material is from the Muséum national d’Histoire naturelle, Paris (MNHN); and some other comparative specimens are housed at the Muséum d’histoire naturelle de la Ville de Genève (MHNG), Academy of Natural Sciences of Drexel University, Philadelphia (ANSP) and the United States National Museum of Natural History, Smithsonian Institution, Washington, DC (USNM). The specimens had been fixed in 70% ethanol. One female of *D. miran* was examined after the shell had been broken in order to complete the extraction of soft parts. In the remaining specimens, extraction was carried out by pulling tissue with forceps to obtain only the soft parts from the last whorl. Study of the visceral mass was precluded. The specimens were dissected by standard techniques under a stereo-microscope while immersed in ethanol. All drawings were made with the aid of a camera lucida. Scanning electron microscopy under a Phillips XL 30 was used to study the radulae, with the usual coating, at the Laboratório de Microscopia Eletrônica, Museu de Zoologia da USP, and Museo Argentino de Ciencias Naturales “Bernardino Rivadavia” (MACN). For the main terminology, including that relating to odontophore muscles, see Simone (2011).

In the figures, the following abbreviations are used: *aa*, anterior aorta; *ad*, adrectal sinus; *af*, afferent gill vessel; *ag*, albumen gland; *an*, anus; *ao*, posterior aorta; *au*, auricle; *bc*, bursa copulatrix; *bg*, buccal ganglion; *br*, subradular membrane; *bs*, buccal sphincter; *ce*, cerebral-pleural ganglia; *cg*, capsule gland; *cm*, columellar muscle; *cv*, ctenidial vein; *dd*, duct to digestive gland; *df*, dorsal fold of buccal mass; *dg*, digestive gland; *di*, diaphragmatic membrane separating haemocoel from visceral cavity; *ea*, anterior oesophagus; *ef*, oesophageal folds; *em*, middle oesophagus; *ep*, posterior oesophagus; *es*, oesophagus; *et*, metapodial tentacles; *ey*, eye; *fp*, female pore; *fs*, foot sole; *ft*, foot; *ga*, aperture of gland of Leiblein; *gc*, cement gland; *gi*, gill or gill filament; *gl*, gland of Leiblein; *ha*, haemocoel; *he*, head; *hg*, hypobranchial gland; *in*, intestine; *ki*, kidney; *kl*, dorsal lobe of kidney; *m1–m14*, extrinsic and intrinsic odontophore muscles; *ma*, longitudinal muscle of odontophore; *mb*, mantle border; *mc*, circular muscles of odontophore; *mf*, muscle fibres; *mo*, mouth; *ne*, nephrostome; *ng*, nephridial gland; *nr*, nerve ring; *nv*, nerve; *oa*, opercular pad; *oc*, odontophore cartilage; *od*, odontophore; *oo*, odontophore tube connecting to oral tube; *op*, operculum; *os*, osphradium; *ot*, oral tube; *oy*, ovary; *pb*, proboscis; *pc*, pericardium; *pd*, penis duct; *pe*, penis; *pg*, anterior

furrow of pedal glands; *ph*, penis terminal or preputial chamber; *pp*, penis papilla; *pt*, prostate; *pu*, pedal ganglion; *py*, pallial cavity; *ra*, radula; *rh*, rhynchostome; *rm*, retractor muscle of proboscis; *rn*, radular nucleus; *rs*, radular sac; *rt*, rectum; *sa*, salivary gland aperture at oral tube; *sc*, subradular cartilage; *sd*, salivary duct; *sf*, siphonal basal flap; *sg*, salivary gland; *si*, siphon; *st*, stomach; *su*, suboesophageal ganglion; *sy*, statocyst; *te* cephalic tentacle; *tg*, integument; *tm*, transverse muscles between oesophagus and odontophore; *vc*, cilia of valve of Leiblein; *vd*, vas deferens; *ve*, ventricle; *vl*, valve of Leiblein; *vo*, visceral oviduct.

TAXONOMY

Genus *Dorsanum* Gray, 1847

Type species *Buccinum politum* Lamarck, 1822 (*non* Röding, 1798) = *Buccinum miran* Bruguière, 1789, by original designation.

Dorsanum miran (Bruguière, 1789)

Figs 1–8, 16, 17, 21–42

Buccinum miran: Bruguière 1789: 268.

Buccinum politum Lamarck, 1822: 269 (*non* Röding, 1789).

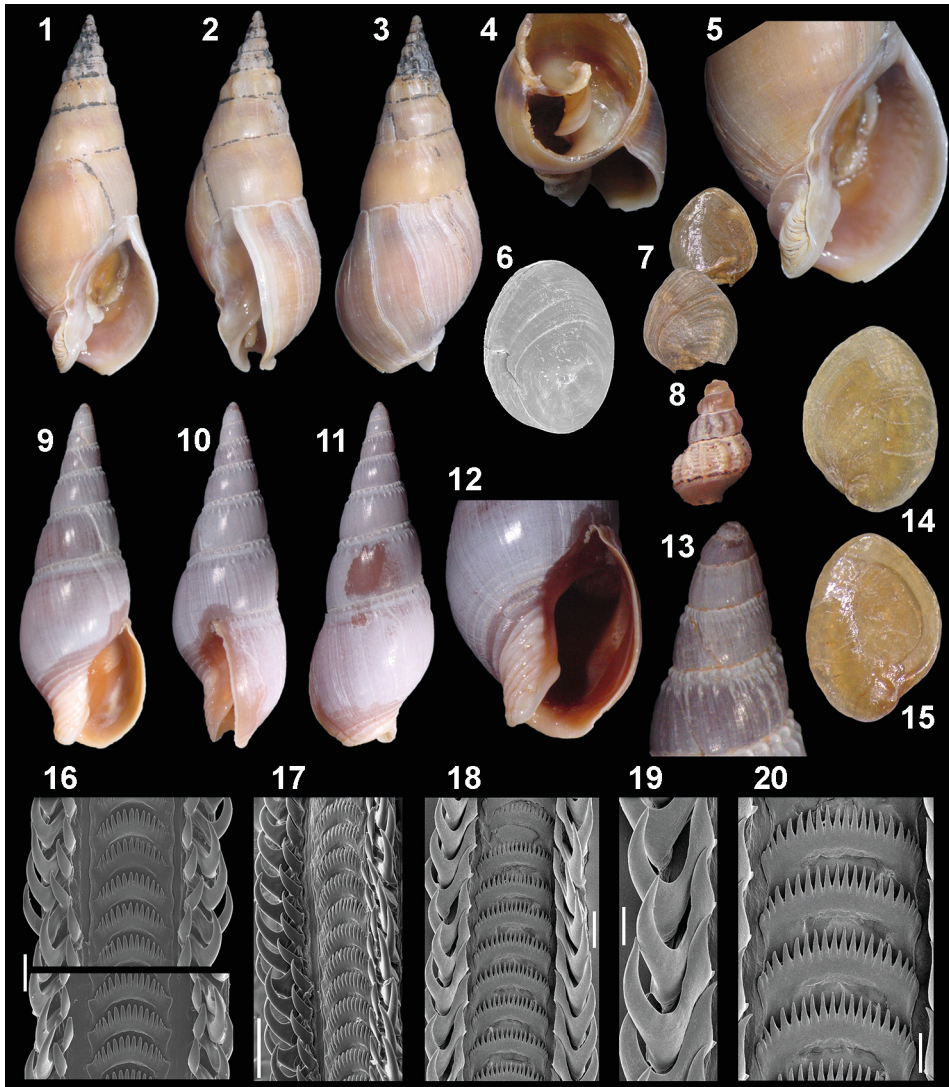
Dorsanum miran: Brebion & Ortlieb 1976: 537–548; Harzhauser & Kwoalke 2004: 34.

Complete synonymy in Fischer-Piette 1942: 160; Cernohorsky 1984: 29; Adam & Knudsen 1984: 69; Allmon 1990: 27.

Description:

Shell (Figs 1–5, 8). Fusiform-elongated. Colour pale brown, with weak spiral, purple subsutural band, opaque; some specimens white-purple. Protoconch elongated, smooth, shining, ~2 whorls; boundary between protoconch and teleoconch well-defined, orthocone (Fig. 8). Spire pointed, ~1.5 of last whorl. Suture shallow but well-marked. Teleoconch of 7 whorls; first 4 whorls with axial varices, ~10 in 4th whorl, gradually disappearing after 6th whorl; among varices 5–6 weak cords slightly protruding when crossing varices in the first 2 whorls only (Fig. 8), gradually disappearing in 3rd whorl. Remaining whorls smooth, opaque, except for growth lines (Figs 1–3, 5). Umbilicus absent. Aperture oval, pale brown, glossy (Figs 1, 5). Siphonal canal short and broad, approximately half of aperture width, left edge truncate, right edge wanting, as continuation of outer lip; left edge marked by two strong spiral folds, superior fold smooth, with sharp edge, inferior fold broad, with several arched, strong growth scales (Fig. 5). Outer lip simple, sharp, rounded (Fig. 2). Inner lip simple, callus narrow, covering right surface of canal. Columella possessing strong spiral folds, located between middle and inferior thirds of each whorl (Fig. 4), ending as right edge of left canal wall, producing small protuberance located between middle and inferior thirds of inner lip (Fig. 5).

Head-foot (Figs 21–25). Head protruded, socket-like (Figs 25, 30: *he*), wide (~80% of head-foot width), colour pale cream with minute dark brown pits scattered on tentacles and head. Tentacles well-separated from each other; elongated and narrow, eyes placed on small protuberances at mid level of tentacle, on small ommatophore; proximal half of tentacles about double the width of distal half (Figs 21, 24, 25). Rhynchostome present as longitudinal slit located in middle region of head's ventral surface (Fig. 25: *rh*). Foot broad, size about half a whorl when retracted. Sole oval, edges thick and rounded (Fig. 22: *fs*). Anterior furrow of pedal glands deep, superior and inferior edges thick, extending



Figs 1–20. SEM of shells, opercula and radulae: (1–8) *Dorsanum miran*; (1) shell, apertural view (length 22.9 mm); (2) right view; (3) dorsal view; (4) apical, slightly apertural view, broken shell showing columellar fold; (5) apertural view, detail of last whorl; (6) outer SEM view of operculum (4.0×3.0 mm); (7) operculum of shell in Fig. 1, inner (upper) and outer views (3.8×3.5 mm); (8) detail of extracted protoconch, profile; (9–15) *Bullia granulosa*; (9) shell, apertural view (length 29.4 mm); (10) right view; (11) dorsal view; (12) apertural view, detail of last whorl; (13) detail of shell apex in profile; (14) operculum, outer view (4.7×3.4 mm); (15) same, inner view; (16–17) *D. miran* radula, scale bar = 100 μ m; (18–20) *B. granulosa* radula; (18) wide view, scale bar = 100 μ m; (19) detail of lateral teeth, scale bar = 50 μ m; (20) detail of rachidian teeth, scale bar = 50 μ m.

to a little beyond anterior edge of foot (Figs 21, 22: *pg*); pedal gland embedded in pedal musculature (Fig. 23: *pg*). One pair of small metapodial tentacles located in posterior end of foot, originating in dorsal region of edge (Fig. 24: *et*). Opercular pad elliptical, ~80%

as wide as dorsal surface of foot; attachment with operculum occupying ~70% of its area (Fig. 24: *oa*). Columellar muscle thick, ~1.5 whorl; distal end bifid, with right element wide, left element narrow, encased in furrow formed by columellar fold (Figs 21, 24: *cm*). Female with small orifice of cement gland located on median line of anterior sole region (Fig. 22: *gc*); inner space wider than narrow duct (Fig. 23: *gc*).

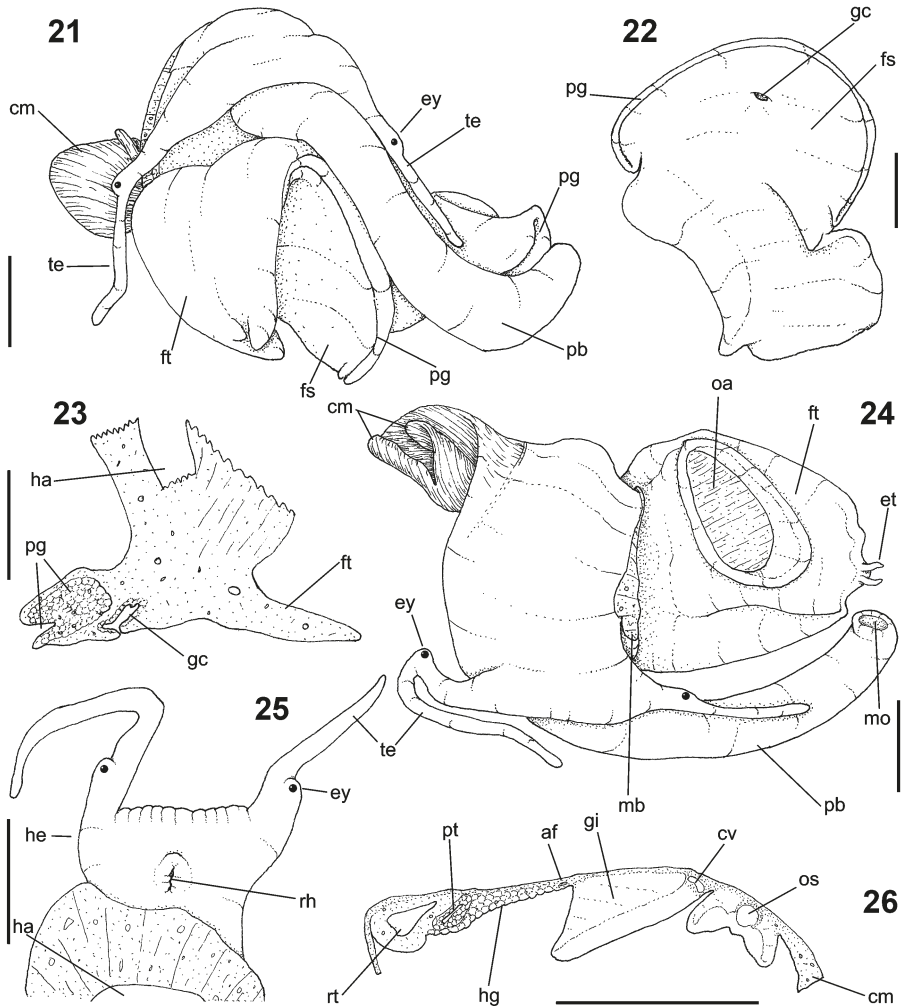
Operculum (Figs 1, 6, 7). Elliptical, horny, pale brown. Nucleus terminal, inferior. Outer surface with normal concentric growth lines, forming undulations. Scar oval, occupying about $\frac{2}{3}$ of inner surface, somewhat dislocated closer to inner edge.

Mantle organs (Figs 26–28). Mantle edge simple, thick. Siphon long, extending beyond mantle edge for 3–4× its base width (Fig. 28: *si*). Low, broad fold of siphon's right base separates anterior end of osphradium and gill. Osphradium ~ $\frac{1}{4}$ width and length of pallial cavity; anterior end pointed, strongly curved towards left; posterior end rounded; osphradium filaments symmetrical, long, bluntly pointed, basal edge reinforced by wide rod (Fig. 26: *os*). Area between osphradium and gill very narrow. Ctenidial vein (*cv*) narrow, width uniform along its length. Gill (*gi*) ~80% of pallial cavity length and ~ $\frac{1}{2}$ its width; anterior end broadly pointed, located at some distance from mantle edge. Afferent gill vessel very narrow, lying at a short distance from right edge of gill (Fig. 26: *af*). Gill separated from right edge of pallial cavity by an area equivalent to its width. Hypobranchial gland thin, beige, covering most of area between gill and rectum, including left and ventral surfaces of rectum (Fig. 26: *hg*). Rectum narrow, with thick walls, running along right edge of pallial cavity (Fig. 26: *rt*). Anus simple, siphoned, located in front of anterior quarter of pallial cavity (Figs 28, 36: *an*). Pallial gonoducts located between rectum and right pallial edge, described below.

Visceral mass (Figs 28, 40). Anterior quarter of whorl mostly occupied by kidney (*ki*) and pericardium (*pc*). Digestive gland beige, located along inferior region of each visceral whorl, covering middle digestive tubes and also two whorls posterior to stomach. Gonad pale beige, lying along superior and columellar surfaces of visceral whorls posterior to stomach. Stomach small, located half a whorl in front of pallial cavity (Fig. 40: *st*).

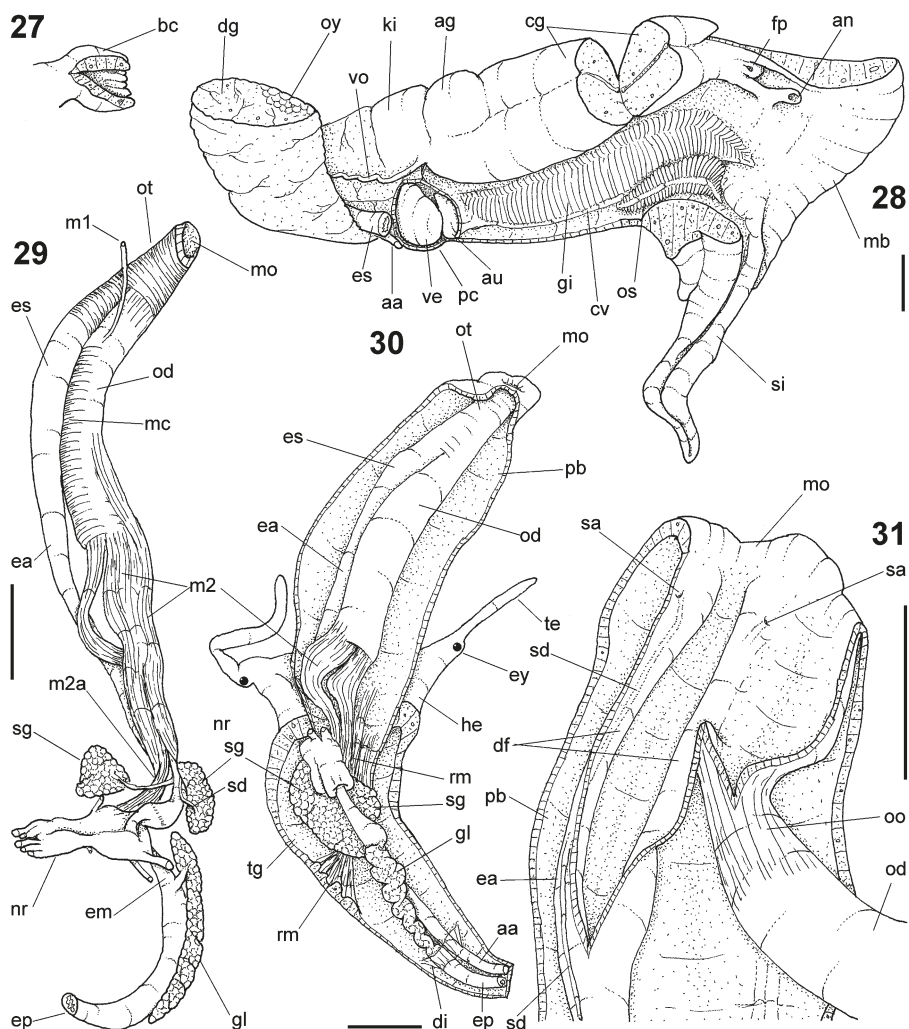
Circulatory and excretory systems (Figs 28, 40). Pericardium (*pc*) located just posterior to gill, along left anterior region of visceral mass. Auricle (*au*) small, triangular, attached to anterior surface of pericardium, with ctenidial vein entering from left and connected to kidney at its right end. Auricle connected to anterior surface of ventricle. Ventricle (*ve*) very large, filling most of pericardium. Aortas located along postero-left region of ventricle. Kidney occupying ~ $\frac{1}{8}$ of pallial cavity, located along middle and right regions of anterior end of visceral mass. Nephridial gland triangular in section; lying along dorsal region of reno-pericardial wall. Renal lobe transversely folded, occupying most of kidney's interior volume (Fig. 40: *ki*); intestine runs through it.

Digestive system (Figs 29–35). *Proboscis* as long as foot (Figs 21, 24: *pb*). Mouth circular, on proboscis tip (Figs 24, 29–31: *mo*). Buccal cavity with a pair of broad and low dorsal folds (Fig. 31: *df*), occupying ~ $\frac{1}{3}$ of dorsal wall, with equivalent distance between them. Odontophore oval, ~70% of length of proboscis (Figs 29, 30: *od*). Odontophore tube connects it with buccal cavity, length equivalent to ~ $\frac{1}{4}$ of odontophore length, possessing mostly longitudinal muscles (Figs 29, 31: *oo*). *Odontophore muscles* (Figs 29–35): *ml*, several small muscle fibres connect buccal mass to adjacent inner surface of proboscis, one more developed pair originating in peribuccal lateral region of proboscis,



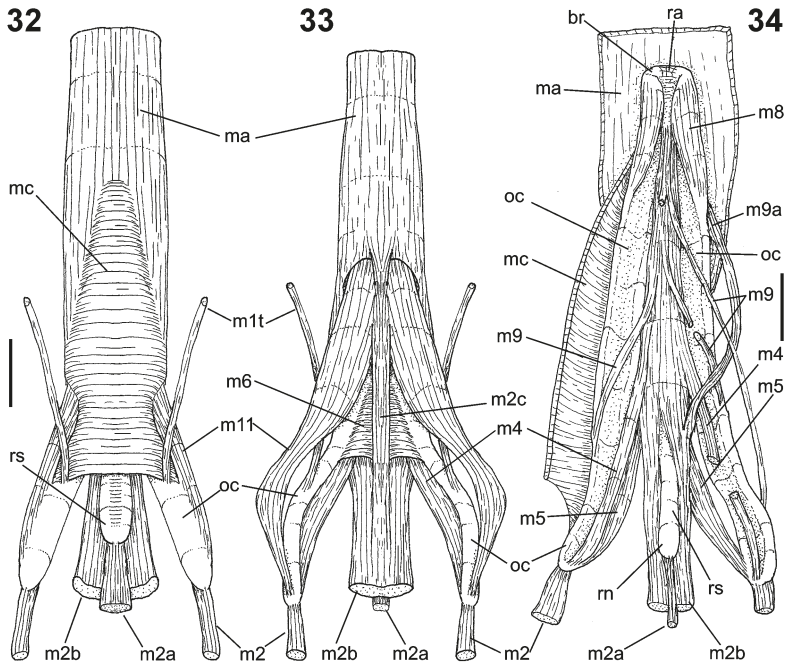
Figs 21–26. *Dorsanum miran* anatomy: (21) head-foot, female, anterior view, specimen with extended proboscis; (22) same, foot sole, ventral view; (23) same, longitudinal section through median line; (24) same, dorsal whole view; (25) head, ventral view, foot extracted; (26) pallial cavity roof, transverse section at mid-level of osphradium. Scale bars = 2 mm.

running posteriorly, inserting in lateral side of anterior third of odontophore (Fig. 29: *m1*); *m1t*, pair of narrow, lateral, transverse protractor muscles of odontophore, originating in lateral region of proboscis, running posteriorly and penetrating membrane surrounding odontophore, inserting in odontophore cartilage in region just posterior to *m6* (Figs 32, 33); *ma*, peribuccal muscles and protractor of odontophore bearing longitudinal fibres, origin thin within dorsal wall of oral cavity, running along odontophore tube and becoming thicker, inserting into outer surface of cartilages externally to *m6* and medially to *m4* (Figs 32–34); *mc*, single, circular constrictor muscle converting dorsal surface of odontophore, inserting along outer side of dorsal edge of cartilages at along ~80% their length (Figs 32, 34); *m2*, main pair of retractor muscles of odontophore, relatively



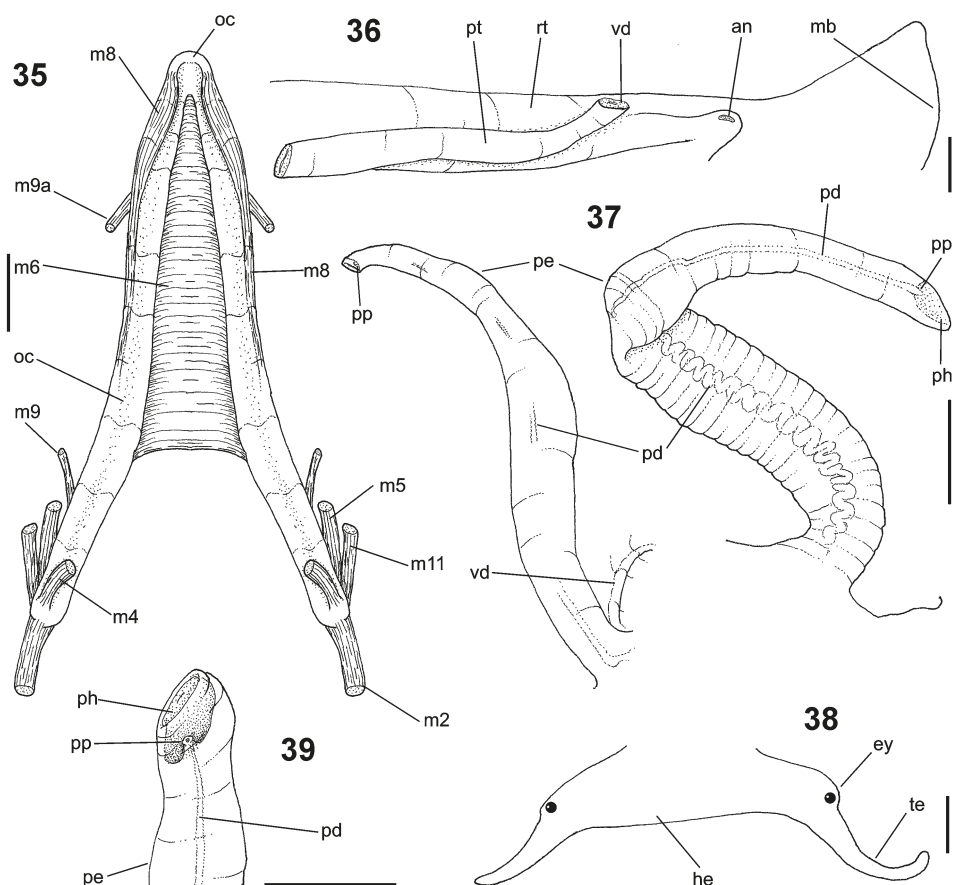
Figs 27–31. *Dorsanum miran* anatomy: (27) detail of anterior end of pallial oviduct, ventral view, partially sectioned longitudinally; (28) pallial cavity roof and adjacent region of visceral mass, inner ventral view, ventral wall of pericardium removed, transverse section of pallial oviduct also shown; (29) foregut, right view, topology of nerve ring also shown; (30) head and haemocoel, ventral view, foot removed, proboscis opened longitudinally; (31) buccal mass, detail of its anterior end opened longitudinally, odontophore partially deflected. Scale bars = 2 mm.

narrow, originating in ventral surface of haemocoel in region just posterior to proboscis, running dorsally, with median fibres running through nerve ring, inserting into posterior end of cartilages (Figs 29, 30, 32–35); *m2a*, auxiliary of *m2*, being single and running between both *m2* muscles, inserting on radular nucleus together with small branch of aorta (Figs 32–34); *m2b*, broad and thick auxiliary pair of *m2* and dorsal tensor muscles of radula, originating as *m2*, running more medially, inserting along radular sac in its mid-region (Figs 32–34); *m2c*, ventral single, thin muscle auxiliary of *m2*, originating on ventral medial fibres of *m2a*, detaching from it in region just posterior to *m6*, runs



Figs 32–34. *Dorsanum miran* odontophore: (32) whole dorsal view, superficial membranes removed; (33) same, ventral view; (34) dorsal muscles *mc* and *ma* sectioned longitudinally and deflected, some narrow muscles also deflected and some sectioned transversely. Scale bars = 1 mm.

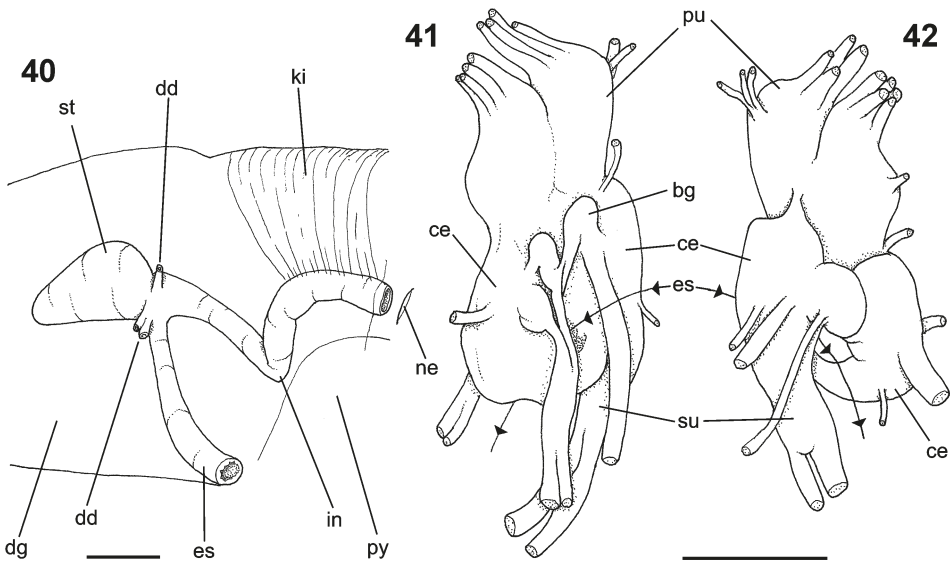
covering medial region of *m6*, inserting on median-posterior region of *ma* (Fig. 33); *m4*, strong pair of dorsal tensor radular muscles, originating in odontophore cartilages on posterior-ventral surface, running towards dorsal surrounding lateral surface of cartilages, inserting laterally along radular sac (Figs 33–35); *m5*, pair of secondary dorsal tensor muscles of radula, originating in posterior-dorsal surface of cartilages, running dorsally and medially, joining with *m4*, inserting into radular sac alongside and medial to *m4* insertion (Figs 33–35); *m6*, thin horizontal muscle, uniting both odontophore cartilages just posterior to anterior fusion for about 70% of cartilage length, inserting along ventral and internal edge of cartilages, gradually becoming broader posteriorly (Figs 33, 35); *m8*, a pair of thick cartilages shorten muscles, which are located along dorsal edge of anterior region of cartilages for almost half their length, being thicker anteriorly and gradually narrowing posteriorly (Figs 34, 35); *m9*, one or two pairs of very narrow protractor muscles of radula, originating on posterior half of dorsal edge of cartilages, running forwards medially, inserting along *m2a* anterior fibres (Figs 34, 35); *m9a*, pair similar to *m9*, originating in anterior region of ventral edge of cartilages, just centrally to posterior region of *m8*, running medially and dorsally, inserting together with *m2b* fibres at level anterior to radular nucleus (Figs 34, 35); *m11*, pair of ventral tensor muscles of radula, thin, somewhat broad, originating in posterior-ventral end of cartilages, running anteriorly and medially covering *m6*, inserting into ventral edge of radula and subradular cartilage, and some inner portions in front of this (Figs 32–35). Subradular cartilage expands in exposed region of radula into buccal cavity, covering



Figs 35–39. *Dorsanum miran* anatomy: (35) odontophore cartilages and adjacent part of intrinsic muscles, showing their origins, dorsal view; (36) right side of pallial cavity, male, ventral view; (37) penis *in situ*, deflected upwards, dorsal view, inner structures revealed by artificial translucence; (38) head and uncoiled penis, dorsal view, adjacent region of penis base also shown; (39) penis, dorsal view, detail of its apical region, inner structures revealed by artificial translucence. Scale bars = 1 mm.

neighbouring surface of radula; *oc*, odontophore cartilages, elongate, furrow-like, flat, $\sim 20\times$ longer than wide; fusion between both cartilages in anterior-medial end, along $\sim 5\%$ of their length (Fig. 35); subradular membrane covers inner surface of subradular cartilage and radula, m4, m5 and m11a insertions.

Radula (Figs 16, 17): *rachidian* tooth wide, comb-like, occupying about half of radular width; curved base, width $\sim 5\times$ greater than its length; ~ 17 triangular, sharp pointed cusps of similar size, except for some diminishment towards the side; *lateral tooth* hook-like, bicuspid, base broad (equivalent to $\frac{1}{2}$ of rachidian base width), obliquely disposed; main lateral cusp widely curved inwards, about as long as base; secondary, medial cusp approximately half the size of lateral cusp; both cusps separated from each other by smooth area equivalent to $\frac{1}{3}$ of tooth's width. *Salivary glands* cluster around oesophagus along region of valve of Leiblein and ventral ganglia of nerve ring, attached to lateral surface of anterior oesophagus just anterior to valve of Leiblein (Figs 29, 30: *sg*);



Figs 40–42. *Dorsanum miran* anatomy: (40) last whorl of visceral mass, ventral view, stomach seen *in situ*, renal region also shown; (41) nerve ring, dorsal view, oesophageal passage indicated by arrows; (42) same, ventral view. Scale bars = 1 mm.

their ducts very narrow, except for short proximal region that runs completely attached to anterior oesophagus wall and, more anteriorly, inside dorsal folds of buccal cavity (Fig. 31: *sd*); opening is a very small pore (Fig. 31: *sa*), into anterior-middle region of dorsal folds of buccal cavity. *Anterior oesophagus* with somewhat thick walls, a little longer than proboscis; inner surface with 12–15 narrow, uniform longitudinal folds. *Valve of Leiblein* about $\frac{1}{12}$ of odontophore volume, anterior region with transverse, white band bearing long cilia, middle and posterior regions white, corresponding to inner gland that occupies most of inner surface; oblique furrow (bypass) absent (Fig. 29: *vl*). *Middle oesophagus* ~10% of anterior oesophagus length (Fig. 29: *em*), walls thin; inner surface similar to that of anterior oesophagus; aperture of gland of Leiblein is a minute pore. *Gland of Leiblein* narrow and elongated (Figs 29, 30: *gl*), ~3× longer than middle oesophagus; anterior region approximately double the length of middle oesophagus width, becoming gradually narrower towards posterior. Duct of gland of Leiblein short and narrow (about 3× shorter than middle oesophagus, and about half of its diameter) (Fig. 29). *Posterior oesophagus* (Figs 29, 30, 40: *ep*) about as long as anterior oesophagus, inner surface with 12–15 narrow, tall, irregular, sometimes coalescent longitudinal folds. *Stomach* oval, blind sac, ~ $\frac{1}{4}$ width of adjacent visceral whorl; located about half a whorl posterior to pallial cavity, positioned approximately in the middle (Fig. 40: *st*). Oesophageal insertion and intestinal origin united in anterior, left side of stomach, additionally having 3 narrow ducts to digestive gland in the same region (Fig. 40: *dd*). Inner gastric surface mostly smooth. *Intestine* about as wide as posterior oesophagus; sigmoid visceral loop (Fig. 40: *in*) is in digestive gland, with region in front of rectum passing through ventro-left side of kidney. Rectum and anus described above (pallial cavity).

Genital system. Male (Figs 36–39). Visceral structures not seen in detail. Prostate spans about $\frac{1}{3}$ of pallial cavity length, narrow, closed (tubular), lying ventrally to rectum (Fig. 36: *pt*). In region posterior to anus, vas deferens gradually crosses to pallial cavity floor, narrow; walls relatively thick, running relatively straight up to penis base (Fig. 38: *vd*). Penis slender, about as long as pallial cavity, its length $\sim 15\times$ greater than its width, dorso-ventrally flattened (Figs 37, 38); base narrow, located just posterior to right tentacle; middle level twisting, narrowing gradually up to bluntly pointed tip (Fig. 37). Penial duct runs approximately along centre of penis, very narrow, intensely coiled in basal half, somewhat straight in distal half (Fig. 37: *pd*). Penial aperture apical, very small, inside wide preputial chamber (Figs 37, 39: *ph*), aperture in middle region of chamber's basal surface, as small papilla (Fig. 39: *pp*); preputial chamber occupying $\frac{1}{30}$ of penis volume, its aperture wide, inclined to the right (Fig. 39).

Female (Figs 27, 28). Visceral oviduct very narrow, running along middle region of columellar surface of last whorl of visceral mass, located in front of pallial cavity by $\sim \frac{1}{4}$ whorl (Fig. 28: *vo*). Posterior region of pallial oviduct protrudes into kidney. Albumen (whitish – *ag*) and capsule (beige – *cg*) glands adjacent, albumen gland spanning posterior $\frac{1}{5}$ of pallial oviduct. Seminal receptacle absent. Capsule gland with flat lumen, vaginal furrow runs along its left edge, with smooth surface (Fig. 28: *cg*). Female pore narrow, weakly protruded, papilla-like, with thick edges (Fig. 28: *fp*). Bursa copulatrix located as terminal portion of pallial oviduct, small, short; with thick muscular walls (Fig. 27: *bc*); its aperture turned ventro-anteriorly as female pore (Fig. 28: *fp*); inner surface with low, wide, longitudinal folds. Cement gland in pedal sole described above (head-foot) (Figs 22, 23: *cg*).

Central nervous system (Figs 41, 42). Well-concentrated, connectives and commissures indistinct; total nerve ring volume $\sim \frac{1}{20}$ of haemocoel. No distinction between pleural and cerebral ganglia (*ce*). Cerebral ganglia broadly connected to each other; commissure approximately half the length and width of each cerebro-pleural mass. Pedal ganglia (*pu*) slightly smaller than cerebro-pleural ganglia; pedal commissure broad, indistinct. Cerebro-pedal and pleuro-pedal connectives short, indistinguishable. Pair of buccal ganglia (*bg*) small, located close to posterior edge of cerebral ganglia. Suboesophageal ganglion (*su*) the size of about half the cerebro-pleural ganglion, shortly and broadly connected to right cerebral ganglion (Fig. 42).

Measurements of shells. MNHN: 1 ♀: 22.9×9.8 mm; 2 ♂: 23.1×9.9 mm.

Distribution: West African coast, from Morocco, Western Sahara, Mauritania, Senegal, Ivory Coast and Gabon (Adam & Knudsen 1984; Allmon 1990).

Habitat: Sandy bottoms, ~ 15 m depth.

Material examined: 1 ♂ 2 ♀ MOROCCO: Agadir Bay; Qued Sours, off Sousse River estuary, $30^{\circ}22'N$ $09^{\circ}37.9'W$, 15 m depth, (Radial I; sandy bottoms, Moukrin & Gofas col. 08.v.1999), MNHN. SENEGAL: ANSP 34627, several shells; Dakar, USNM 617323, 1 shell.

Type remarks: Cernohorsky (1984) illustrated a syntype of *Buccinum politum* housed at the MHNG (1101/99) and one syntype of *Buccinum miran* after Fischer-Piette (1942) from the MNHN.

Genus *Bullia* Gray in Griffith & Pidgeon, 1834

Type species *Bullia semiplicata* Gray, 1834 = *B. callosa* (Wood, 1828), by original designation.

Bullia granulosa (Lamarck, 1822)

Figs 9–15, 18–20, 43–55

Terebra granulosa Lamarck, 1822: 291.

Complete synonymy in Cernohorsky 1984: 28; Adam & Knudsen 1984: 66 and Allmon 1990: 28.

Description:

Shell (Figs 9–13). Similar to preceding species. Differences: Color uniform bright purple-beige; aperture brown. Protoconch wider (Figs 9–11), occupying $\sim\frac{1}{8}$ of shell width in adult forms, dome-shaped, of two whorls (Fig. 13); boundary between protoconch and teleoconch unclear. Sculptured, with axial threads in first teleoconch whorl (Fig. 13), two series of subsutural nodes in remaining whorls, each node axially elongated, those closer to suture slightly smaller; growth lines in the rest of whorl. Region at left of aperture possessing ~ 8 spiral cords, somewhat uniformly distributed in left side of inner lip and canal (Figs 9, 10, 12), inferior cords slightly narrower than superior cords. Inner lip with small protuberance in base of canal (Fig. 12).

Head-foot (Figs 43, 44, 47). Characters similar to those of preceding species, including socket-like head (Fig. 44), bifid columellar muscle (Fig. 43: *cm*), and pair of small metapodial tentacles (Fig. 43: *et*). Differences: Head somewhat narrower, without eyes. Female lacking detectable cement gland at foot sole.

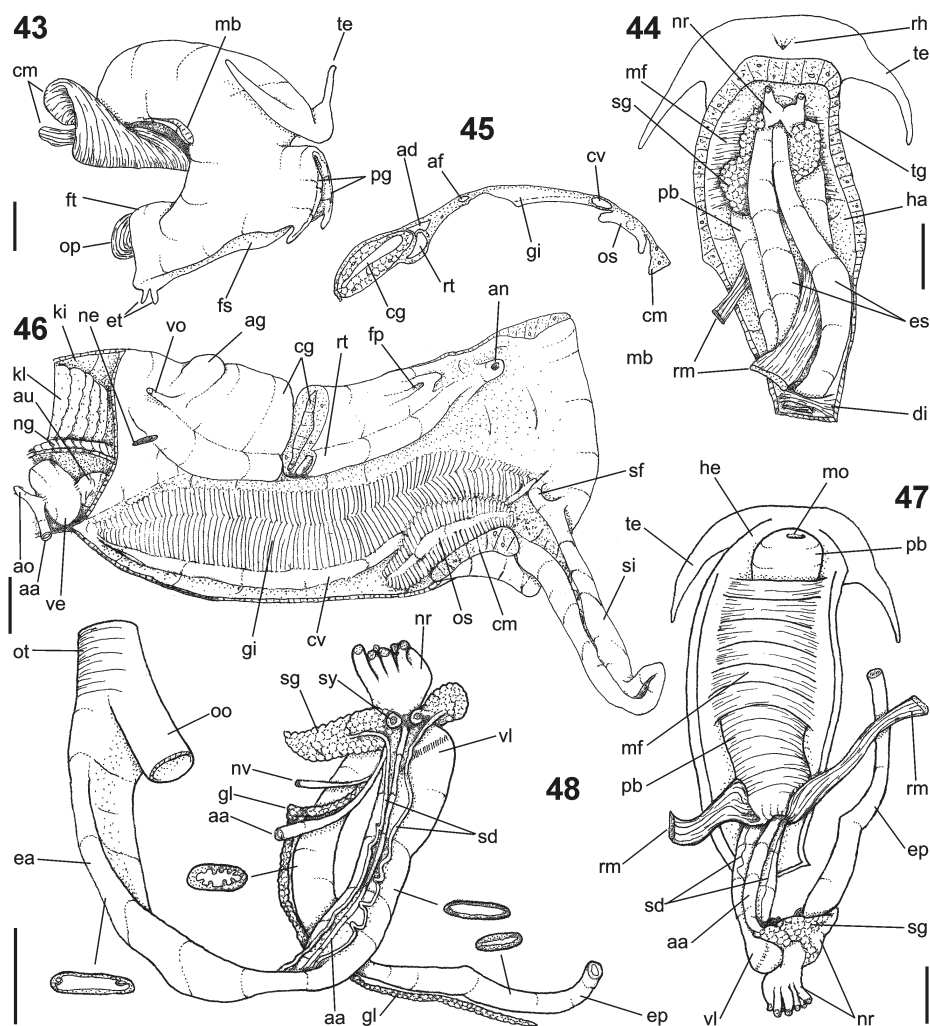
Operculum (Figs 14, 15). Elliptical, horny, pale brown. Nucleus inferior, subterminal but close to inferior edge. Outer surface with normal concentric growth lines, forming undulations. Scar oval, occupying about $\frac{1}{2}$ of inner surface, somewhat dislocated closer to inner edge; flanked by strong and wide ridge in outer edge (Fig. 15).

Mantle organs (Figs 45, 46). Similar to those of preceding species. Remarks and differences: Low, broad fold of siphon's right base separates anterior end of osphradium from gill and is somewhat taller (Fig. 46: *sf*). Osphradium (*os*) with filaments shorter, but with longer lateral projections (Fig. 45: *os*). Ctenidial vein (*cv*) relatively broader, weakly expanded at mid-level. Gill with much shorter filaments, apex approximately at mid-level (Fig. 45: *gi*). Anus shortly siphoned, located in front of anterior $\frac{1}{5}$ of pallial cavity (Fig. 46: *an*).

Visceral mass. Not seen in detail.

Circulatory and excretory systems (Fig. 46). Similar to preceding species, except that the dorsal side of the renal lobe is more developed (*kl*).

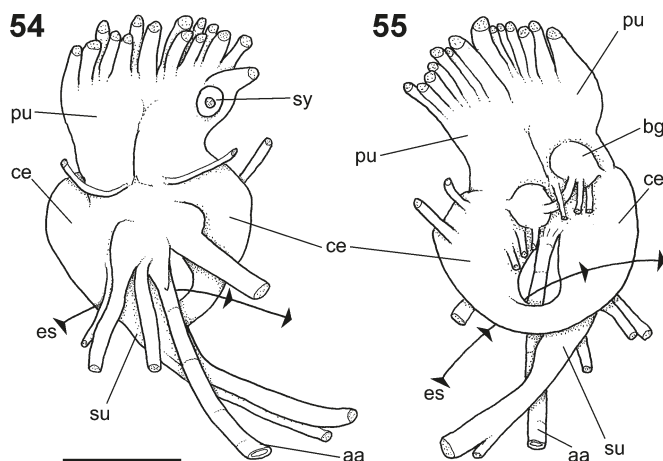
Digestive system (Figs 47–53). Main features and general plan similar to those of preceding species. Remarks and differences: *Proboscis* with similar arrangement, but possessing stronger transverse muscle, covering both ventral surface of rhynchodeal wall (Fig. 47: *mf*), and between oesophagus and odontophore in buccal mass (Fig. 49: *tm*). Odontophore proportionally shorter, $\sim 50\%$ of length of proboscis (Fig. 49: *od*). *Odontophore* muscles with similar arrangement (Figs 50, 52, 53), except for: *m1*, no especially developed jugal muscle; *mc*, somewhat longer, reaching $\sim 90\%$ of length of cartilages up to region close to their posterior end (Figs 52, 53); *m2b*, originating as 4–5 branches, uniting themselves in region before entrance in odontophore (Fig. 52); *m2c*, slightly broader (Figs 50, 52); *m2d*, pair of auxiliary muscles of *m2b*, running externally, with same origin, inserting jointly with *m2b* (Figs 50, 52); *m4*, pair slightly broader (Fig. 52); *m6*, thin horizontal muscle, about 80% of cartilage length (Figs 52, 53); *m9*, similar,



Figs 43–48. *Bullia granulosa* anatomy: (43) head-foot, female, right view; (44) head and haemocoel, ventral view, foot and columellar muscles removed; (45) pallial cavity roof, transverse section in mid-level of osphradium; (46) same, whole ventral view, transverse section in pallial oviduct artificially done, adjacent portion of visceral structures also shown; (47) foregut, ventral view, topology of some adjacent structures shown; (48) same, right view, proboscis and odontophore extracted. Scale bars = 2 mm.

but only present as a single pair (Fig. 52); *m9a*, much more developed, about as wide as *m4*, broadly covering radular nucleus (Figs 52, 53). Subradular cartilage expanded in exposed region of radula into buccal cavity (Fig. 50: *sc*), covering neighbouring surface of radula; *oc*, odontophore cartilages similarly fashioned, except for greater extent of fusion, along ~10% their length (Fig. 53).

Radula similar to that of preceding species (Figs 18–20): *rachidian* with ~21 cusps and thinner; base of the rachidian less curved; *lateral tooth* also similar, with inner cusp rising from base being more pronounced (Fig. 19). *Salivary glands* with similar features,



Figs 54–55. *Bullia granulosa* anatomy of nerve ring, topology of oesophagus indicated by arrows: (54) dorsal view; (55) ventral view. Scale bar = 1 mm.

except for their ducts, with clear expansion in region in front of their aperture, situated within dorsal folds of buccal cavity (*df*), and salivary aperture more laterally positioned (Fig. 49: *sa*). *Anterior oesophagus* much broader, about as broad as odontophore (Figs 48, 49: *ea*). *Valve of Leiblein* also broader (Fig. 48: *vl*), with well-developed inner cilia (Fig. 51: *vc*). *Middle and posterior oesophagus* with similar characters (Figs 48, 51: *em*, *ep*). *Gland of Leiblein* very narrow, elongated, filiform (Figs 48, 51: *gl*); $\sim 3\times$ longer than middle oesophagus and $\sim 10\times$ narrower than it; twisted between anterior and middle thirds, just in region where aorta passes (Figs 48: *aa*). Duct of gland of Leiblein almost undetectable, aperture simple (Fig. 51: *ga*). Stomach and intestine not examined in detail. Rectum and anus described above (pallial cavity).

Genital system. Male. No male was available for examination.

Female (Fig. 46). General features similar to those of preceding species; except for relatively shorter albumen gland (*ag*) and female pore (*fp*) being situated further away from anus. No cement gland detectable.

Central nervous system (Figs 54, 55). Similar to that of preceding species, except for narrower commissure of buccal ganglia (Fig. 55: *bg*), and longer commissure between cerebral ganglia. Statocyst located in antero-ventral region of pedal ganglia (*sy*).

Measurements of shells. MNHN 1♀: 29.4 × 10.7 mm.

Distribution: From Morocco to Democratic Republic of the Congo.

Habitat: Sandy bottoms, ~ 15 m depth.

Material examined: 1♀, 1 shell: MOROCCO: Agadir Bay; Qued Sours, off Sousse River estuary, 30°22'N 09°37.9'W, from 15 m depth, MNHN, (Radial I; sandy bottoms, Moukrin & Gofas col. 08.v.1999).

DISCUSSION

Although there is no doubt about the validity of both species, the shells of *Dorsanum miran* and *Bullia granulosa* are so similar that they are commonly found together in the same lot in collections, as if the shells are those of a single species. Only after more

detailed study of both shells and anatomy did the specific and even generic distinctions become apparent. The main shell differences include the apex, which is more sharply pointed in *D. miran* than in *B. granulosa* (compare Figs 1–3 with 9–11). The sculpture is also different in that *D. miran* has some broad nodulation in the first teleoconch whorl (Figs 1–3), whereas *B. granulosa* has a delicate pair of subsutural nodes extending all along the whorls (Figs 9–11). The sculpture of the region to the left of the aperture is also dissimilar, as *D. miran* has only a single pair of broad folds (Fig. 5), and *B. granulosa* has 7–8 delicate ones (Fig. 12). The protuberance in the canal's left base, almost a tooth, is well-developed in *D. miran* (Fig. 5) but weaker in *B. granulosa* (Fig. 12); it is at the end of the columellar fold (Fig. 4) in the former, a feature that was not confirmed for the latter because the shell could not be broken.

The main anatomical differences and similarities were incorporated into the distinctive description of *B. granulosa*. The absence of eyes in *B. granulosa* (Figs 43, 44) clearly separates this species from *D. miran*, where the eyes are very characteristic (Figs 24, 25). The fold of the siphonal base separating the anterior end of the osphradium from the gill in *B. granulosa* (Fig. 46: *sf*) is taller than in *D. miran* (Fig. 28). The gill and osphradium filaments are much larger in *D. miran* (Fig. 26) than in *B. granulosa* (Fig. 45). The transverse musculature of the haemocoel is much more developed in *B. granulosa* than in *D. miran* in the ventral rhynchodeal wall (Fig. 47: *mf*) and between the oesophagus and odontophore (Fig. 49: *tm*). As regards odontophore muscles, the multiplicity of m2b that creates the pair m2d (Fig. 52) in *B. granulosa* is the main distinctive feature, this muscle being much simpler in *D. miran*. That aside, the pair m9a of *B. granulosa* are enlarged (Fig. 52). All these features indicate that *B. granulosa* has stronger odontophore musculature than *D. miran*. The extent of fusion between both odontophore cartilages is greater in *B. granulosa* (Fig. 53) than in *D. miran* (Fig. 35). Moreover, the anterior oesophagus and valve of Leiblein of *B. granulosa* are proportionally broader in *B. granulosa* (Fig. 48) than in *D. miran* (Fig. 29). Both species have in common a somewhat reduced gland of Leiblein. However, that of *B. granulosa* is elongated and filiform (Fig. 48: *gl*) as compared with the “usual” form exhibited by *D. miran* (Fig. 29). Related to the nerve ring, *B. granulosa* has the cerebral and buccal commissures longer than those of *D. miran* (Figs 42, 55), but both are very concentrated as in all buccinoid nerve rings (Bailey 1966).

The marked conchological similarity between *D. miran* and *B. granulosa* has been pointed out in the literature. Allmon (1990: 28, 29) invoked anatomical studies to resolve the taxonomy. In fact, several characters allow the specific and even generic distinctions to be made, as reflected above. However, knowledge based on additional species is necessary for a more complete taxonomical evaluation. Despite *B. granulosa* having been used here as representative of the genus *Bullia*, it is important to emphasize that the type species, *B. callosa*, still needs to be studied. Generic inferences can then be made in the light of such an assessment.

Allmon (1990) erected the subfamily Bulliinae in his revision of the so called “*Bullia* group”, for which he studied mostly fossil representatives from North America. He mentioned the uncertain generic position of *B. granulosa* and several other genera. In his diagnosis of the subfamily, he included mainly shell characters, comparing Bulliinae with Dorsaninae and Nassariinae. Whereas those characters are clear when representatives of the Nassariinae are compared, they are not easy to see in Dorsaninae. He mentioned

as main shell differences in Bulliinae the lack of a recurved siphonal channel with a carina on the dorsal side of the fasciole, and the reduced ornamentation.

The diagnostic features are the large size for a nassariid, considering that some species attain a shell length of 100 mm, such as *Buccinanops cochlidium* (Dillwyn, 1817), while the typical nassariid is approximately 10 mm. The absence of a well-developed callus is another exclusivity, this structure being particularly robust in most nassariids. The callus and a more developed sculpture of the typical nassariids generate a thicker shell wall. The lack of or reduction in these features produces the thinner shell typical of the *Bullia* group. In general, the shells of the species so far included in the *Bullia* group resemble those of the Buccinidae more closely than shells of nassariids.

In regard to anatomy, the tendency for the gland of Leiblein to be reduced and the simplification of the female pallial oviduct are noteworthy attributes in comparison with the situation in other buccinoideans (Fretter 1942; Haasl 2000; Kantor & Harasewych 2008; Kosyan *et al.* 2009). The nassariid nature of the *Bullia* group species comes from the socket-like head and the metapodial tentacles, which are paired in both examined species, but single in *Buccinanops* (Simone 1996). The term “socket-like” for the head was coined by Marcus and Marcus (1962), and means a head that protrudes in a form that resembles an electric socket, in which the tentacles are the pins.

The nerve rings of both species are closely similar (Figs 41, 42, 54, 55), highly concentrated in such a way that the pleural and cerebral ganglia cannot be distinguished from each other. This is an accepted feature for a neogastropod (Fretter 1942). However, the cerebral commissure is somewhat long in both species studied. The concentration of ganglia and the closure of the buccal ganglia has been referred to for another allied species, *Bullia digitalis* (Dillwyn, 1817) (Brown 1982, figs 16A, B), as well as the protuberances on opposite sides of the buccal ganglia (Figs 42, 54), which have been termed the sub and supra-intestinal ganglion, respectively (Brown 1982). They are not so distinct in the presently studied species, however. Conversely, the elongated suboesophageal ganglion close to the nerve ring, present in both species (Figs 41, 54: *su*), is not shown by Brown (1982) for *B. digitalis*.

An interesting feature is the absence of eyes, which is typical for *Buccinanops*. This trait is shared with *B. granulosa*, but not with *D. miran*, which has well-developed eyes (Fig. 25). On the other hand, the reduced gland of Leiblein of the anatomically known *Buccinanops* resembles more closely that of *D. miran*.

The elongated odontophore of both examined species is typical for buccinoideans (Wilsmann 1942; Simone 1996, 2011), including the main features of the muscles and cartilages. The degree of cartilage fusion and the length of the horizontal muscles (m6) are, by contrast, smaller in both examined species (Figs 35, 53). The pair or pairs of protractor muscles of the radula, here called m9, is so far another exclusivity, but a more detailed assessment of these and other odontophore characters will be needed in the future, in comparison with *Buccinanops*.

B. granulosa has previously been assigned to the genus *Dorsanum*, more precisely the subgenus *Fluviadorsum* Boettger, 1885 (Cernohorsky 1984). However, since no character fully agrees with that classification, we have kept the species in the genus *Bullia*, following most previous authors.

Although the original intention was to improve upon the definition of nassariid subfamilies, as set out by Allmon (1990), by providing anatomical details, is it still

unclear whether the differences outlined above have validity as distinguishing characters at the specific, generic or subfamilial level. Discussion in this regard is accordingly postponed to a time when the anatomy of more species has become better known. A phylogenetic analysis will then be feasible; and this will be the next step in this ongoing investigation.

ACKNOWLEDGEMENTS

We are grateful to Philippe Bouchet and Virginie Heros (MNHN) for lending material to us; to Lara Guimarães (MZSP) for helping with the SEM examination; and to Yuri Kantor, Igor Muratov and an anonymous referee for text improvement. This contribution was supported in part by Fapesp (Fundação de Amparo à Pesquisa do Estado de São Paulo) projects 2004/10793-9, 2006/02524-3, and 2010/02285-4.

REFERENCES

- ADAM, W. & KNUDSEN, J. 1984. Révision des Nassariidae (Mollusca: Gastropoda, Prosobranchia) de l'Afrique occidentale. *Bulletin de l'Institut Royal des Sciences Naturelles de Belgique, Biologie* **55**: 1–95, pls. 1–5.
- ALLMON, W.D. 1990. Review of the *Bullia* group (Gastropoda: Nassariidae), with comments on its evolution, biogeography, and phylogeny. *Bulletins of American Paleontology* **99** (335): 1–179, 15 pls.
- BAILEY, D.F. 1966. Aspects of the neurophysiology of *Buccinum undatum* L. (Gastropoda). II. Central organisation. *Journal of Experimental Biology* **44**: 149–161.
- BREBION, P. & ORTLIEB, L. 1976. Nouvelles recherches géologiques et malacologiques sur le Quaternaire de la province de Tarfaya (Maroc Méridional). *Géobios* **9**: 529–550.
- BROWN, A.C. 1982. The biology of sandy-beach whelks of the genus *Bullia* (Nassariidae). *Oceanography and Marine Biology, Annual Review* **20**: 309–361.
- BRUGUIÈRE, J.G. 1789. *Encyclopédie Méthodique. Histoire Naturelle des Vers*. Vol. 1. Paris: Panckoucke.
- CERNOHORSKY, W.O. 1984. Systematics of the family Nassariidae (Mollusca: Gastropoda). *Bulletin of the Auckland Institute and Museum* **14**: 1–356.
- FISCHER-PIETTE, E. 1942. Les mollusques d'Adanson. *Journal de Conchyliologie* **85**: 101–366, pls 1–16.
- FRETTER, V. 1942. The genital ducts of some British stenoglossan prosobranchs. *Journal of the Marine Biological Association of the United Kingdom* **25**: 173–211.
- GRIFFITH, E. & PIDGEON, E. 1834. *The animal kingdom arranged in conformity with its organization, by the Baron Cuvier, with additional descriptions of all the species hitherto named, and of many not before noticed. Vol. 12. The Mollusca and Radiata. Arranged by the Baron Cuvier, with supplementary additions to each order*. London: Whittaker.
- HAASL, D.M. 2000. Phylogenetic relationships among nassariid gastropods. *Journal of Paleontology* **74**: 839–852.
- HARZHAUSER, M. & KOWALKE, T. 2004. Survey of the nassariid gastropods in the Neogene Paratethys (Mollusca: Caenogastropoda: Buccinoidea). *Archiv für Molluskenkunde* **133**: 1–61.
- KANTOR, Y.I. & HARASEWYCH, M.G. 2008. *Chlanidota (Paranotofcula) anomala*, a new subgenus and species of Buccinulidae (Gastropoda: Neogastropoda) from the South Shetland Islands. *Ruthenica* **18**: 17–24.
- KOSYAN, A.R., MODICA, M.V. & OLIVERIO, M. 2009. The anatomy and relationships of *Troschelia* (Neogastropoda: Buccinidae): new evidence for a close fasciolariid-buccinid relationship? *Nautilus* **123**: 95–105.
- LAMARCK, J.-B.P.M. 1822. *Histoire naturelle des animaux sans vertèbres*. Tome 6, partie 2. Paris: Verdrière, pp.1–232.
- MARCUS, E. & MARCUS, E. 1962. Studies on Columbelloidea. *Boletim da Faculdade de Filosofia, Ciências e Letras da Universidade de São Paulo*, 261, *Zoologia* **24**: 335–402.
- PASTORINO, G. 1993. The taxonomic status of *Buccinanops* d'Orbigny, 1841 (Gastropoda: Nassariidae). *Veliger* **36**: 160–165.
- RÖDING, P.F. 1798. *Museum Boltenianum*. Hamburg.
- SIMONE, L.R.L. 1996. Anatomy and systematics of *Buccinanops gradatus* (Deshayes, 1844) and *Buccinanops moniliferus* (Kiener, 1834) (Neogastropoda, Muricoidea) from the southeastern coast of Brazil. *Malacologia* **38**: 87–102.
- 2011. Phylogeny of the Caenogastropoda (Mollusca), based on comparative morphology. *Arquivos de Zoologia* **42**: 161–323.
- WILSMANN, T. 1942. Der Pharynx von *Buccinum undatum*. *Zoologische Jahrbücher. Abteilung für Anatomie und Ontogenie der Tiere* **61**: 1–48.